


A Wideband Variable Width Microstrip Grid Array Antenna

Osama Khan, Juan Pontes, Xuyang Li, and Christian Waldschmidt

DOI: 10.1109/EuMC.2014.6986769

A Wideband Variable Width Microstrip Grid Array Antenna

Osama Khan*, Juan Pontes*, Xuyang Li*, and Christian Waldschmidt†
*Engineering Components Radar
Robert Bosch GmbH, Leonberg, Germany
Email: osama.khan@de.bosch.com
†Institute of Microwave Engineering
University of Ulm, Ulm, Germany
Email: christian.waldschmidt@uni-ulm.de

***Abstract*—A wideband planar microstrip grid array antenna is presented. The antenna is realized on a standard Rogers RO3003 substrate. It is fed using two centrally located microstrip vias through a ground aperture. Measured results show a 12% S11 <-10 dB bandwidth and a maximum gain of 17 dBi. Using a variable microstrip line width, a side-lobe suppression of at least -12 dB between 77-85 GHz is measured. The antenna can be used in short and medium range operation for automotive radar.**

***Keywords*—Grid array, millimeter-wave antennas, microstrip antennas**

I. Introduction

In recent years, there has been a rise in demand in commercial applications using millimeter-wave frequencies. Millimeter wavelengths allow a physically smaller antenna design, coupled with an increased absolute frequency bandwidth. Multiple applications use this frequency range due to these advantages. Highly directional radio links as well as automotive radar are examples of such applications. The frequency range 77-81 GHz has been allocated to short and medium range radar applications [1]. Automotive radar sensors are being employed in driver assistance systems where they are used in applications such as blind spot detection, collision warning, and pedestrian safety. As these driver assistance systems become ubiquitous in the middle and low-price automobile segment, the demand for high performance and low cost radar sensors will increase significantly.

Antenna performance is an important factor in determining the overall radar sensor performance. Different antenna concepts have been implemented in millimeter automotive radar [2]. Microstrip planar antenna concepts provide a cost-effective option with compact size and low profile for easier vehicle integration. Conventional microstrip antennas however, such as the patch antenna, suffer from low impedance bandwidth. This limits their frequency range of operation. One of the alternative microstrip antenna concepts is the grid array antenna.

The grid antenna was first reported in literature by Krauss [3] who introduced it as a backward angle-fire antenna. The array was fed from one side, resulting in a squinted beam radiated perpendicular to the plane of the grid. Conti et. al [4] realized it in microstrip technology. The microstrip grid array antenna in different configurations has been studied extensively. Nakano et. al [5] integrated a central feed which results in a broadside antenna pattern. Recently Zhang et al. [6] and Bauer et. al. [7] have implemented the microstrip grid array antenna for millimeter-waves on low temperature co-fired ceramics (LTCC) substrates, and standard soft substrate [8]. Depending on the configuration used, these antennas provide a high maximum gain and wide impedance bandwidth.

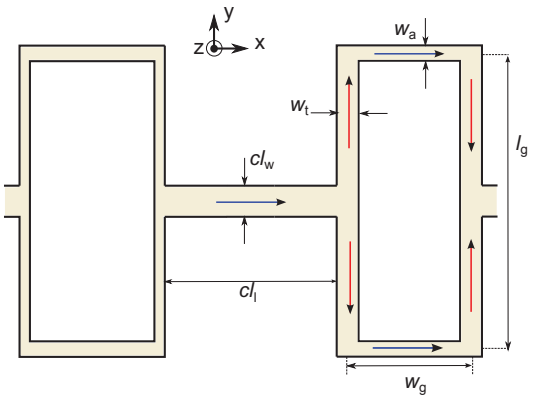

Figure 1: Grid element dimensions and instantaneous current

This paper presents a microstrip grid array antenna designed on Rogers RO3003 substrate. This configuation of the grid antenna is a linear array that results in a high gain narrow beam in the E-Plane and a wide beam in the H-Plane. The highlight of this paper is an enhanced antenna pattern stability and side lobe suppression even beyond the intended operating frequency range of 77-81 GHz. This paper is organized as follows: Section II describes the design procedure of the antenna array. First the single grid element is presented, followed by the array design and feed network design. Section III provides measurement results. Finally, the conclusion is provided in Section IV.

II. Design procedure

The grid array is realized by first designing a single rectangular grid element on a Rogers RO3003 substrate layer ($h = 0.254$ mm, $\epsilon_r = 3$) and then extending the design procedure to the complete array. Afterwards, the feeding method as well as power distribution network is implemented.

A. Single element design

The radiation properties of a rectangular grid element can be understood by analyzing the current flow on the microstrip lines that make up the grid. The single rectangular loop is shown in Fig. 1, with a length $l_g \approx \lambda_g$ and width $w_g \approx \lambda_g/2$. Here, $\lambda_g = \lambda_0/\sqrt{\epsilon_{eff}}$ is the substrate wavelength, λ_0 and ϵ_{eff} are the free space wavelength and effective dielectric constant respectively at the design center-frequency of operation 79 GHz. The instantaneous currents in the horizontzal lines of the loop as well as the connecting lines cause a horizontally (x-directed) polarized field to radiate, where as the currents in the vertical lines cause a vertically polarized (y-directed) field to radiate. The horizontally polarized components combine constructively, whereas the vertically polarized components cancel each other in the broadside direction. Hence a net horizontally polarized field is radiated in the broadside direction.

B. Array design

The horizontal lines of the rectangular loop in Fig.1 can be considered as the radiating elements of the grid array. As the current through these elements is responsible for the radiation, the widths w_a of these lines determine the radiated power from each element. As suggested in [9] these widths can be taken as a first approximation for the weights of the antenna elements in the array. In [10], the normalized currents, which are inversely proportional to the characteristic impedance of the radiating line, and hence approximately inversely proportional to the line width, are used as the antenna element weights. Hence, a higher current is responsible for increased radiation. There are, however, limits on the realizable element widths due to manufacturing constraints and cross-polarized radiated fields. The lowest possible width of 0.1 mm is dictated by manufacturing process limitations. For line widths exceeding 0.6 mm, a high cross-polarized radiating field was observed. Hence the maximum line width of 0.6 mm was considered.

In this work, an array of 10 rectangular loops was designed. Two-port simulations were carried out in CST [11] with a terminated element, and the line width w_a for each array element was optimized. To obtain a symmetric weighting on the array, the element widths were symmetrically chosen. Furthermore, in order to achieve large weighting coefficients for the central radiating elements, two via feeds on the central elements were employed. Each of these feed points is located at the junction of the connecting line and vertical grid line, with a transmission line a multiple of $\lambda_g/2$ between them. Hence, for broadside radiation, the feeds require a 180° phase difference between them. The grid array antenna, symmetric about the midpoint of the connecting line cl0, is shown in Fig. 2.

Additionally, the transmission line length connecting the radiating elements, determined by the length of the rectangular loop l_g and the connecting line length cl_l, are mainly responsible for the phase difference between the radiating elements, but also on the element weighting and hence the side lobe suppression. These lengths are optimized to obtain a broadside radiating array with low side lobe levels. A shorting via with diameter 0.3 mm was also placed at both ends of the array to improve the impedance bandwidth and side lobe suppression over the frequency range of operation.

TABLE I: Dimensions of rectangular loops in mm

Rectangular loop	l_g	w_g	w_a	w_t
L1	2.60	1.15	0.54	0.10
L2	2.50	1.15	0.40	0.10
L3	2.40	1.15	0.30	0.10
L4	2.30	1.15	0.20	0.10
L5	2.30	1.15	0.10	0.10

TABLE II: Dimensions of connecting lines in mm

Dimensions	cl0	cl1	cl2	cl3	cl4
cl_l	1.50	1.30	1.30	1.50	1.50
cl_w	0.30	0.30	0.30	0.30	0.30

The optimized geometrical dimensions of the array are listed in Table I. The lengths of the connecting lines are listed in Table II.

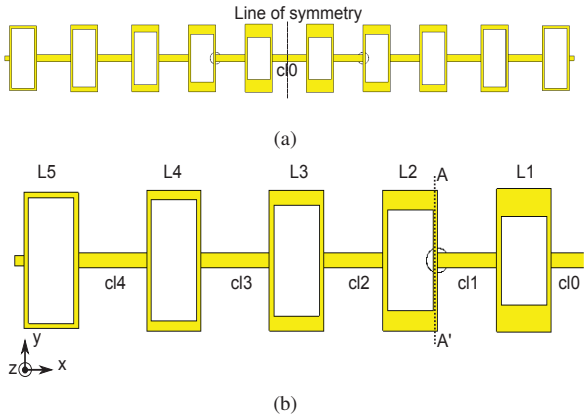

Figure 2: Top complete view (a) and left half view (b) of grid array antenna

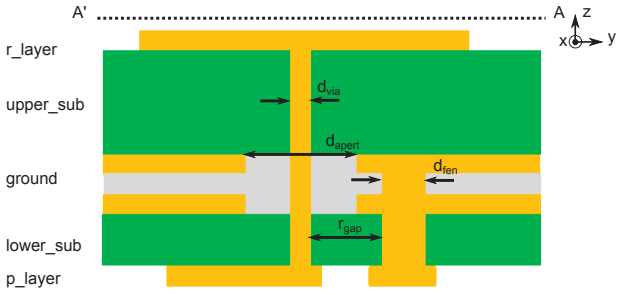

Figure 3: Cross section of antenna at feed-point

C. Feeding network

The vias feed the the antenna structure through a hole in the ground plane. Initially, a coaxial via approach, similar to that in [12] is taken to simulate the antenna performance without the influence of the feeding network. The via diameter d_{via} = 0.12 mm and outer conductor diameter d_{apert} = 0.5 mm is chosen to obtain a coaxial line characteristic impedance of 50 Ω, to which the grid array is matched. The feeding network used was realized on a separate layer of substrate. Here, a 50 Ω transmission line was fed to a 3 dB 180° power divider,

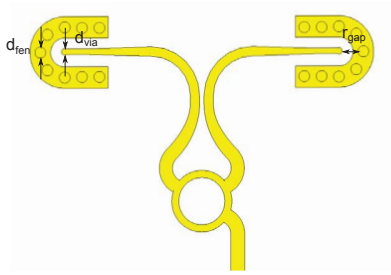

Figure 4: Feed network

whose outputs were then matched to the via by a smooth tapering. Due to manufacturing limitations, feed vias with d_{via} = 0.15 mm and d_{apert} = 0.6 mm were used in the manufactured design.

A via fence was also added around the feed vias to connect the two ground planes. As shown in [13], addition of fencing vias improves the field transition from the microstrip to the coaxial feed modes, and reduces parallel plate modes between the ground planes. Hence, there is a better impedance matching, as well as less distortion due to radiation from the substrate edges. A total of 9 fencing vias with diameter d_{fen} = 250 μm were placed around each feed via at a distance of r_{gap} = 0.36 mm.

The cross section of the final antenna design including the feed structure is shown in Fig. 3. The top radiating layer r_layer with metallization thickness of 18 μm is on the substrate layer upper_sub of height 0.254 mm. It is backed by the two ground layers, which act as the ground plane for the antenna and the power distribution layer p_layer respectively. Each copper layer is 18 μm thick, separated by a bonding film of thickness 100 μm. The feeding network is on the p_layer, which is on top of the substrate layer lower_sub of height 0.127 mm. This makes the total thickness of the antenna, including the feeding layer about 0.550 mm.

III. Measurement Results

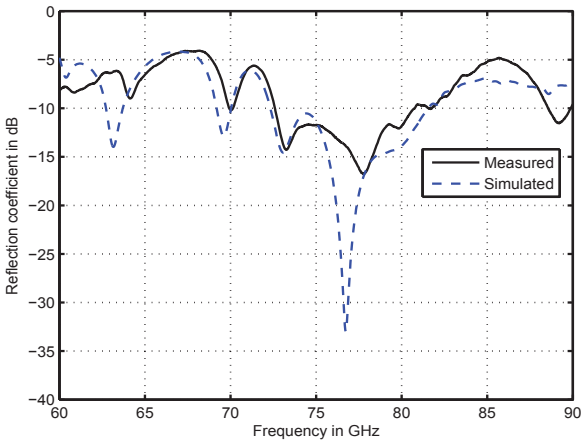

Figure 5: Antenna reflection coefficient

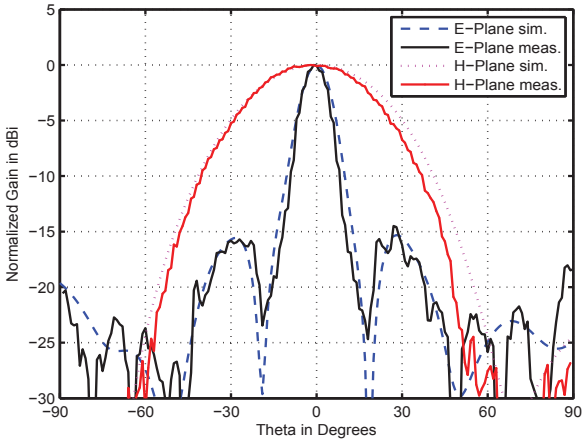

(a)

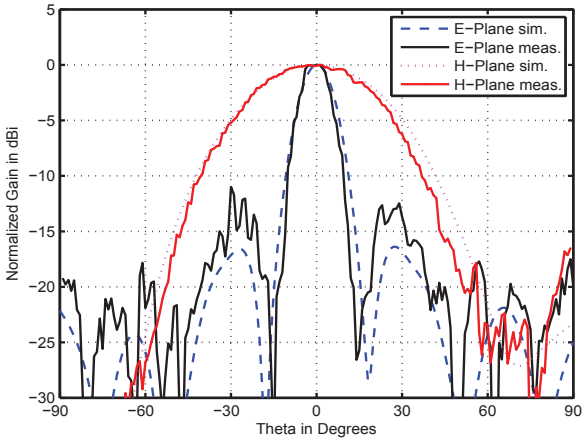

(b)

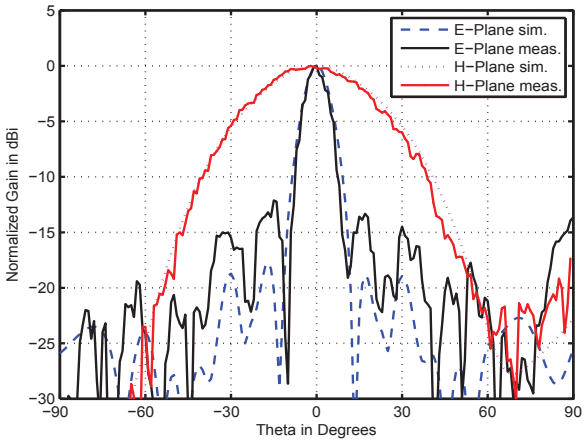

(c)

Figure 6: Normalized radiation pattern of antenna in E-Plane (x-z) and H-Plane (y-z) at (a) 77 GHz (b) 80 GHz and (c) 85 GHz

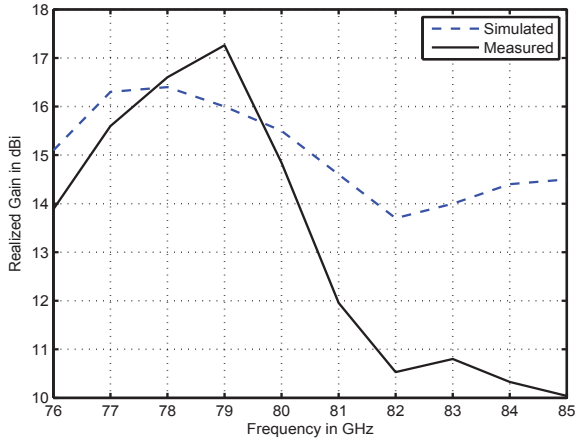

Figure 7: Broadside gain of antenna over frequency

The designed antenna was manufactured and measured to verify the simulation results. For the reflection coefficient measurements, a standard GSG-probe transition was used. For the radiation pattern measurement, the waveguide transition from [14] was used on the power distribution layer. Hence, two different PCBs were manufactured to measure the reflection coefficient and the antenna diagram. The reflection coefficient results are shown in Fig. 5, showing a wideband impedance matching in the frequency range 73-82 GHz (Reflection coefficient <-10 dB) for about 12% impedance bandwidth.

The normalized simulated and measured co-polarized farfield radiation diagrams at 77 GHz, 80 GHz and 85 GHz are shown in Fig. 6. It can be seen that the antenna pattern remains stable over this frequency range. A 3 dB gain beamwidth of 10° in the E-Plane and 44° in the H-Plane are measured respectively at 77 GHz. Hence, the array provides a high gain narrow beam in the E-Plane, and a wide field of view in the H-Plane. The lowest side lobe level of -15 dB in the E-plane is achieved at 77 GHz, with the side-lobe level at -12 dB at 85 GHz.

Broadside realized gain over frequency is shown in Fig. 7. The maximum measured gain is 17.2 dBi at 79 GHz. For frequencies greater than 80 GHz, a deviation between measured and simulated realized gain is observed. Possible reasons for this are the mismatch losses at frequencies above 80 GHz at the waveguide transition, or at the antenna input. For high-gain operation, the antenna can be used over a frequency range of about 4 GHz. Operating ranges of up to 9 GHz are possible with adequate side lobe suppression in the E-Plane, albeit with reduced gain.

IV. Conclusion

A microstrip grid array antenna, realized on a low profile Rogers RO3003 substrate was presented. The antenna is fed using microstrip vias and employs a separate power distribution layer. Using variable widths of radiating elements, optimum amplitude tapering across the antenna array is achieved. The measured results show a wideband impedance bandwidth and a stable antenna pattern coupled with adequate side lobe suppression throughout the operating frequency range. Possible applications of this antenna are the medium and short range radar from 77 GHz to 81 GHz, with a high gain in elevation plane, and a wide field of view in the azimuth plane.

References

[1] European Commission: Commission Impelementing Decision 2011/485/EU of 29 July 2011 amending Decision 2005/50/EC on the harmonisation of the 24 GHz range radio spectrum band for the time-limited use by automotive short-range radar equipment in the Community (notified under document C(2011) 5444). Official Journal of the European Union L 198/71, (2011).

[2] W. Menzel and A. Moebius, "Antenna concepts for millimeter-wave automotive radar sensors," *Proceedings of the IEEE*, vol. 100, no. 7, pp. 2372–2379, July 2012.

[3] J. Kraus, "A backward angle-fire array antenna," *Antennas and Propagation, IEEE Transactions on*, vol. 12, no. 1, pp. 48–50, 1964.

[4] R. Conti, J. Toth, T. Dowling, and J. Weiss, "The wire grid microstrip antenna," *Antennas and Propagation, IEEE Transactions on*, vol. 29, no. 1, pp. 157–166, 1981.

[5] H. Nakano, I. Oshima, H. Mimaki, K. Hirose, and J. Yamauchi, "Center-fed grid array antennas," in *Antennas and Propagation Society International Symposium, 1995. AP-S. Digest*, vol. 4, 1995, pp. 2010–2013 vol.4.

[6] B. Zhang and Y. P. Zhang, "Grid array antennas with subarrays and multiple feeds for 60-GHz radios," *Antennas and Propagation, IEEE Transactions on*, vol. 60, no. 5, pp. 2270–2275, 2012.

[7] F. Bauer and W. Menzel, "A 79 GHz microstrip grid array antenna using a laminated waveguide feed in LTCC," in *Antennas and Propagation (APSURSI), 2011 IEEE International Symposium on*, 2011, pp. 2067–2070.

[8] M. Frei, F. Bauer, W. Menzel, A. Stelzer, and L. Maurer, "A 79 GHz differentially fed grid array antenna," in *Radar Conference (EuRAD), 2011 European*, Oct 2011, pp. 432–435.

[9] K. Palmer and J. Cloete, "Synthesis of the microstrip wire grid array," in *Antennas and Propagation, Tenth International Conference on (Conf. Publ. No. 436)*, vol. 1, 1997, pp. 114–118 vol.1.

[10] L. Zhang, W. Zhang, and Y.-P. Zhang, "Microstrip grid and comb array antennas," *Antennas and Propagation, IEEE Transactions on*, vol. 59, no. 11, pp. 4077–4084, Nov 2011.

[11] CST MICROWAVE STUDIO ®, Release Version 2013.01 - May 16 2013, CST AG. [Online]. Available: cst.com

[12] F. Bauer, X. Wang, W. Menzel, and A. Stelzer, "A 79-GHz radar sensor in LTCC technology using grid array antennas," *Microwave Theory and Techniques, IEEE Transactions on*, vol. 61, no. 6, pp. 2514–2521, June 2013.

[13] B. Zhang, D. Titz, F. Ferrero, C. Luxey, and Y. P. Zhang, "Integration of quadruple linearly-polarized microstrip grid array antennas for 60-ghz antenna-in-package applications," *Components, Packaging and Manufacturing Technology, IEEE Transactions on*, vol. 3, no. 8, pp. 1293–1300, Aug 2013.

[14] E. Topak, J. Hasch, and T. Zwick, "Compact topside millimeter-wave waveguide-to-microstrip transitions," *Microwave and Wireless Components Letters, IEEE*, vol. 23, no. 12, pp. 641–643, Dec 2013.